International Journal of Applied Pharmaceutics

ISSN- 0975-7058 Vol 16, Special Issue 6, 2024

Original Article

RESEARCH ON MECHANISM OF SHENLING BAIZHU SAN ON DIABETIC OBESITY BASED ON META-ANALYSIS AND NETWORK PHARMACOLOGY

XIAOLING ZHOU, LIPING TANG, DIYAO WU, XINYOU ZHANG*

Jiangxi University of Chinese Medicine, Nanchang, Jiangxi, China
***Corresponding author: Xinyou Zhang; *Email: xinyouzhang@163.com**

Received: 19 Mar 2024, Revised and Accepted: 10 Sep 2024

ABSTRACT

Objective: To evaluate the therapeutic effects of Shenling Baizhu San on diabetic obesity by literature meta-analysis and analyze the mechanism of Shenling Baizhu San on diabetic obesity by combining network pharmacology and animal experiment methods.

Methods: 1. Relevant literatures at home and abroad were included. The BMI, glycosylated hemoglobin (HbA1c), 2h postprandial blood glucose (2hPG), Fasting Blood Glucose (FBG), Homa-IR, waist-to-hip ratio were used as outcome indicators to evaluate the effects of Shenling Baizhu San on diabetic obesity. 2. The related genes of diabetes obesity in GEO chip were downloaded, and the targets of Shenling Baizhu San were downloaded in TCMSP, TCMID and BATMAN-TCM. Protein interaction analysis was carried out on the intersection targets of the two, and then the core target protein was screened out based on topological analysis. 3. The model of diabetic obese mice was established, and the mice were treated with Shenling Baizhu San after grouping. After two weeks, the body mass, blood sugar and Lee's index of mice in each group were measured. The volume changes of adipocytes in each group were analyzed by Hematoxylin-Eosin method, and the concentrations of cholesterol, triglyceride and core target protein in mice serum were measured.

Results: 1. A total of 9 literatures were included, the data were complete, no publication bias was found, and the evaluation was low risk. After administration of Shenling Baizhu San, the BMI, HbA1c, 2hPG, FBG, Homa-IR and waist-hip ratio of the patients were significantly improved. 2. There were 337 genes related to diabetes obesity, 2067 targets of Shenling Baizhu San and 59 intersecting targets. There were 7 signal pathways related to the effect of Shenling Baizhu San on diabetes obesity, including Biosynthesis of unsaved fatty acids, Fatty acid metabolism and so on. 3. The results of animal experiment showed that the blood glucose of mice treated with Shenling Baizhu San was not significantly changed, the body weight and Lee's index showed a significant downward trend, the fat cells were significantly reduced, and the contents of cholesterol and triglyceride, the concentration of APO-E, IGF-1 and PAI-1 protein showed a downward trend.

Conclusion: Based on the results of meta-analysis and animal experiments, Shenling Baizhu San had obvious therapeutic effect on diabetic obesity, and its mechanism may be related to influencing the synthesis of unsaturated fatty acids and fatty acids, reducing the transformation of glucose and fat, correcting the imbalance of energy metabolism in the body, and promoting the decomposition of adipose tissue by up-regulating autophagy.

Keywords: Shenling baizhu san, Diabetes obesity, Mechanism, Meta-analysis, Network pharmacology

DOI: https://dx.doi.org/10.22159/ijap.2024.v16s6.SE2020 Journal homepage: https://innovareacademics.in/journals/index.php/ijap

INTRODUCTION

Obesity or overweight has long been considered as an independent risk factor for various diseases, including hypertension, coronary heart disease, especially diabetes [1]. A series of active factors secreted by adipose tissue is able to induce insulin resistance, and thus result in affecting glucose metabolism [2]. Therefore, obesity combined with diabetes is extremely common in clinical practice. Insulin resistance caused by obesity will further progress to metabolic syndrome, leading to the occurrence of diabetic Cardio Vascular Disease (CVD), which poses a serious threat to human health [3] and has become a global public health problem [4, 5].

From the perspective of Traditional Chinese Medicine (TCM), diabetic obesity is mainly due to the usual addiction to fat diet and sweetness, prolonged sitting and multiple lying, resulting in spleen deficiency and loss of transport and transformation. In modern clinical practice, numerous studies have confirmed that [6-7] traditional Chinese medicine has definite curative effect in treating diabetes obesity, especially the compound Chinese medicines for invigorating spleen and eliminating dampness, such as Shenling Baizhu San (SLBZS) and Jianpi Xiaozhi Decoction, which have been clinically proved to not only reduce the patient's weight but also assist in controlling the development of diabetes [8, 9]. Nevertheless, its specific mechanism of action has not yet been studied clearly. The present study aims to evaluate the therapeutic effect of SLBZS on diabetic obesity through literature meta-analysis, and then analyze the mechanism of SLBZS on diabetic obesity in combination with network pharmacology and animal experiments so as to promote its application in diabetic obesity and improve the clinical cure rate and safety of diabetic obesity.

MATERIALS AND METHODS

The overall flow chart of this paper is shown in fig. 1.

Meta-analysis

Literature inclusion criteria

- The Randomized Controlled Trial (RCT) published at home and abroad;
- All the subjects were in line with the diagnostic criteria for diabetes, including Chinese Guidelines for Prevention and Treatment of Type 2 Diabetes (2017 Edition) and Guidelines for Prevention and Control of Overweight and Obesity in Chinese Adults.
- All the subjects had no other concomitant diseases, and there was no statistical difference in baseline data.

Literature exclusion criteria

(1) Documents did not meet the inclusion criteria;

(2) Animal, review, and repetitive publications;

(3) Documents containing other intervention measures and comorbidities;

(4) Documents with incomplete or incorrect test information and inconsistent design;

Outcome indicators

BMI, glycosylated hemoglobin (HbA1c), 2h postprandial blood glucose (2h PG), Fasting Blood Glucose (FBG), Homa-IR, waist-hip ratio.

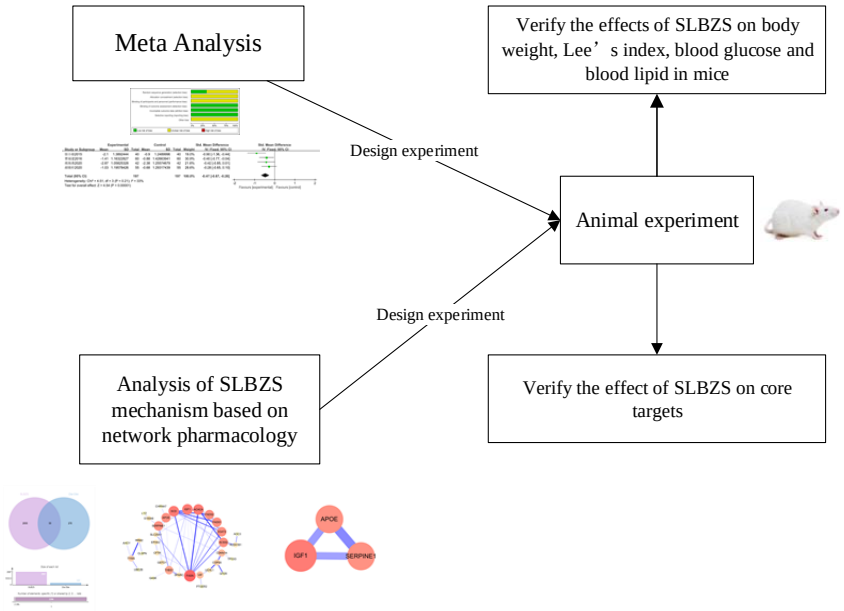

Fig. 1: Flow chart of the mechanism of SLBZS on diabetes obesity based on Meta and network pharmacology

Literature retrieval strategy

With "diabetes and obesity" and "Shen ling Bai zhu San" as the subject words, the relevant literatures were searched in CNKI, VIP, WANGFANG and CBM. With "diabetes obesity" and "Shen ling Bai zhu San/powder" as the subject words, the relevant literatures were searched in PubMed and web of science databases. The time was from the construction of the database to June 2021.

Literature screening and quality evaluation

Data extraction: Two evaluators with professional knowledge background of evidence-based medicine independently screened the literatures and excluded the literatures which obviously did not meet the inclusion criteria. After that, the two evaluators exchanged the results and checked the documents and data extracted from the documents. If there are differences in opinions between the two parties, another professional evaluation is required until the final opinions are reached.

Evaluation of literature quality: According to Cochrane Manual of Evidence-based Medicine, the bias risk of systematic evaluation results from was evaluated based on the aspects of random sequence generation, distribution concealment and the integrity of outcome data.

Statistical processing: Meta-analysis was carried out on the data extracted from the literature by using RevMan5.3 analysis software. The ratio (OR) was taken as the relative effect index variable of counting data, and the Standardized mean Difference (SMD) or mean Difference (MD) was taken as the relative effect index of measuring data. The effect value and its 95% Confidence Interval (CI) were taken as the index of the reliability of the results. The heterogeneity of results was mainly judged by I2 test. If P>0.10 and I2<50% in the results, the heterogeneity of outcome indicators was small, and the fixed effect model should be adopted for analysis. If P<0.10 and I2>50% in the results, the heterogeneity of the outcome indicators was large, and the random effect model should be adopted for analysis.

Network pharmacological analysis

Disease targets of diabetes and obesity

The obesity gene of diabetes was downloaded from GEO chip (https://www.ncbi.nlm.nih.gov/). During this period, the GEO DateSets was selected on the left side of the search box, "Diabetic Obesity" was searched, and the GSE number, platforms and sample information were recorded. Then, data were analyzed by R language, and the related genes of diabetic obesity were obtained.

Action target of SLBZS

The action targets of SLBZS were obtained from TCMSP (https://old.tcmsp-e.com/tcmsp.php), TCMID (http://119.3.41.228:8000/tcmid/) and BATMAN-TCM (http://bionet.ncpsb.org.cn/batman-tcm/) respectively. After removing the duplicates, the data were integrated to obtain the action targets of SLBZS. Venny diagram was drawn by JVENN net (http://jvenn.toulouse.inra.fr/app/example.html) to get the intersection, which was the action target of SLBZS in treating diabetic obesity.

Core target of SLBZS in treating diabetic obesity

All the targets of SLBZS in treating diabetic obesity were input into String platform (https://www.string-db.org/) for protein interaction analysis, and after removing unconnected targets, the network diagram of protein interaction was obtained. Then, the network diagram was input into Cytoscape_v3.8.2, and APP--cytoNCA plug-in was selected. Degree Centrality (DC), Closeness Centrality (CC) and Betweenness Centrality (BC) were clicked and screen out the core target of SLBZS in diabetic obesity.

Animal experiment

Experimental mice

Sixty SD mice weighing 20–25g which were provided by Hunan Slake Jingda Experimental Animal Co., Ltd, (Certificate No. SYXK(Gan)2017-0004) were kept in SPF-grade experimental animal houses. The illumination time was from 6:00 to 18:00. All mice were housed under conditions of constant humidity. The mice were fed with standard fodder and water freely. After 7 d of adaptive feeding, the mice were randomly divided into conventional feeding group (ND) and High Fat Feeding Group (HFD), with a ratio of 10:50.

Drugs and reagents

High sugar and high-fat mouse feed was purchased from Nanjing Shengmin animal farm (batch No. 210610); All 10 traditional Chinese medicines contained in Shenling Baizhu powder (White Lentils, Atractylodes, Poria, Licorice, Platycodon, Lotus Seed, Ginseng, Amomum, Chinese Yam, Coix Seed) were purchased from the pharmacy of the Affiliated Hospital of Jiangxi University of traditional Chinese medicine; 4% paraformaldehyde was purchased

from Biosharp company; Anhydrous ethanol was purchased from Sinopharm Chemical Reagent Co., Ltd. (Item No.100092683); Xylene was purchased from Sinopharm Chemical Reagent Co., Ltd. (Item No.10023418); HE matoxylin eosin (He) staining solution was purchased from Beijing Regan Biotechnology Co., Ltd. (Item No. DH 0006); Neutral gum was purchased from Sinopharm Chemical Reagents Co., Ltd. (Item No.10004160). Elisa test boxes for TC, TG, APO-E, IGF-1 and PAI-1 were purchased from Nanjing jiancheng technology Co., Ltd.

Apparatus

Paraffin embedding machine EG1150 (Leica); RM2016 (Leica); Mingmei MF43 microscope (Mingmei); Minmei MC50 Digital Imaging Measurement and Analysis System (Mingmei); Labsystems Finnpipette 100μl single channel pipette; Thermo 50μl 8-channel pipette; HH-4 Digital Display Constant Temperature Water Bath Pot (Guohua Electric Appliance Co., Ltd.); Electronic DG5033A microplate reader (Nanjing Huadong Electronics Group Medical Equipment Co., Ltd.); Blood glucose meter (Sannuo Intelligent Blood Glucose Meter).

Experimental method

Establishment and grouping of diabetic obesity models

In view of the fact that diabetic obesity patients were mostly caused by high-sugar and high-fat diet [10], we adopted dietary induction method to establish the diabetic obesity model. Due to the irregular eating time of mice, it was impossible to determine the blood glucose before and after meals. The diagnostic criteria of diabetes based on fasting plasma glucose or postprandial blood glucose are not applicable to this study. Therefore, the change of blood glucose was selected as the measurement index. The establishment criteria of the model were as follows: the weight of mice in model group ≥ the weight of mice in blank group ×120%, and the blood glucose of mice after modeling ≥ the blood sugar of mice before modeling ×130%. If the criteria were met, it was judged that the model had been successfully established.

Grouping of mice

Fifty mice in high-fat feeding group were randomly divided into model group (high-sugar and high-fat diet) and administration group (high-sugar and high-fat diet+SLBZS) after feeding for 30 d. The administration doses of SLBZS were 0.33g/day (SLBZS-L), 0.66g/day (SLBZS-M) and 1.32g/day, respectively. After two weeks of intragastric treatment, mice were dissected, blood and adipose tissue were collected, and all experimental operations were in compliance with the requirements of the Ethics Committee of Jiangxi University of Traditional Chinese Medicine.

Measurement of body weight and blood sugar

From the modeling period, the body weight of mice was measured every five days, and the blood from the tail tip vein of mice was taken at a fixed time point every five days to measure blood glucose and record the data.

Lee's index measurement

The weight of mice was measured before dissection, the body length (length from nose tip to anus) was measured by straightening, and the Lee's index of each mouse was calculated.

HE staining

After the mice were dissected, the abdominal adipose tissue was taken. After baking, sectioning, dewaxing, dyeing, dehydration, transparency and sealing, the abdominal adipose tissue was observed, photographed and analyzed under eyepieces 40x, 100x and 400x.

Blood lipid analysis

The blood of mouse orbital venous plexus was collected and put into the test tube. After coagulation, the upper serum was taken. The contents of cholesterol and triglyceride in mouse serum were determined by enzyme labeling colorimetry.

Core target analysis

According to the core target results obtained in 1.2.3, the concentration of core target protein in mouse serum was detected by ELISA kit.

RESULTS

Results of meta-analysis

Results of literature retrieval and inclusion

According to the above retrieval strategies, 66 articles were included in total, including 1 PubMed, 18 CNKI, 21 Wanfang, 11 VIP and 15 CBM. After removing duplicates, 26 articles were obtained. After reading the title and abstract, 14 unrelated literatures were deleted, and 2 were deleted after reading the full text. Finally, 9 literatures were obtained, including 3058 patients. The literature screening process and results were shown in fig. 2.

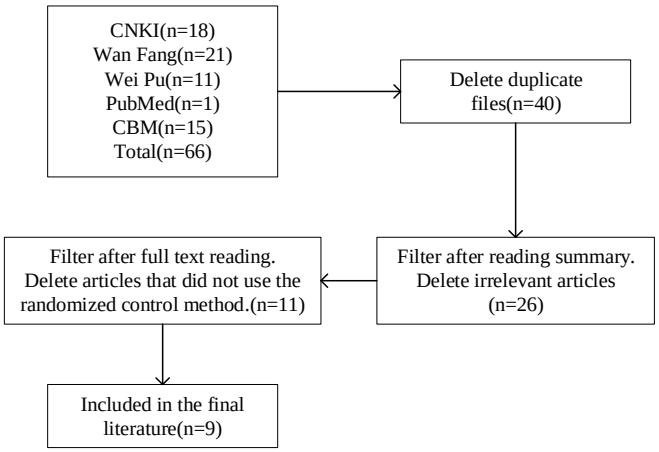

Fig. 2: Screening process of included literature

Basic characteristics of included literature

A total of 9 literatures, 769 patients, were included, including 386 cases in the treatment group and 383 cases in the control group. The outcome indicators mainly included BMI, glycosylated hemoglobin (HbA1c), 2h postprandial blood glucose (2hPG), fasting blood glucose (FBG), Homa-IR, and waist-to-hip ratio. The basic characteristics of the included literature were shown in table 1.

Table 1: Basic characteristics of included literatures

Author	Publication data	Grouping method	Experimental/ control group	Intervention of experimental group	Intervention of control group	Indicators
Peng Junhua [11]	2021	Random number table	43/43	SLBZS+Metformin	Metformin	MiR-146a, GLP-1 and IL-12; Serum TG, TC, LDL-C levels and BMI changes;
Jiang Haiyan [12]	2020	Random	42/42	SLBZS+Metformin	Metformin	The levels of FG, Ins and HbA1c; The amount of bacterial DNA in intestinal flora; Adverse reactions.
Sun Luyang [13]	2020	Random	43/43	SLBZS+Metformin	Metformin	Serological indicators; Correlation between mi R-221 and HOMA-IR and other serological indexes.
Hao Xiaoshan [14]	2020	Random	55/55	Insulin+SLBZS	Insulin	Blood glucose indexes
Chen Zhifang [15]	2019	By computer software, follow the random principle	25/25	SLBZS addition or subtraction+Metformin	Metformin	Blood glucose indexes; Treatment effect
Ma Ningning [16]	2017	Admission sequence number	46/47	Metformin enteric-coated tablets+SLBZS addition or subtraction	Metformin	Blood glucose indexes; Gastrointestinal hormone; Insulin resistance; Fat hormone
Cao Fujian [17]	2016	Random	60/60	Insulin+SLBZS addition or subtraction	Insulin	Blood glucose indexes; Obesity index; adverse effect
Xu Xiaojuan [18]	2015	Random number table	40/40	Insulin+SLBZS addition or subtraction	Insulin	Blood glucose indexes; Obesity index; Adverse effect
Ma Xiu [19]	2015	According to sequence of enrollment	32/28	SLBZS addition or subtraction+Metformin	Metformin	TCM scores; Obesity index; adverse effect; Blood glucose indexes; Adverse effect

Footprint: HbA1c (glycosylated hemoglobin); 2hPG (2h Postprandial blood Glucose); FBG(Fasting Blood Glucose); SLBZS(Sheng Ling Bai Zhu San)

Bias risk assessment of included literature

According to the biased risk assessment method of Cochrane risk assessment table, the quality of 9 included literatures was evaluated, and the evaluation results were described by "low risk", "unclear risk" and "high risk". All the literatures included in this study mentioned random grouping, among which 5 literatures [11, 15, 16, 18, 19] clearly explained the specific random method, which was assessed as low risk; 4 literatures [12-14, 17] only mentioned random grouping, which was assessed as unclear risk; None of the included studies mentioned allocation concealment and blindness, which was assessed as unclear risk; Other biases were unknown, which was assessed as unclear risk; All the literatures had clear outcome indicators and complete data, no publication bias was found, and thus was assessed as unclear risk. The assessment results were shown in fig. 3.

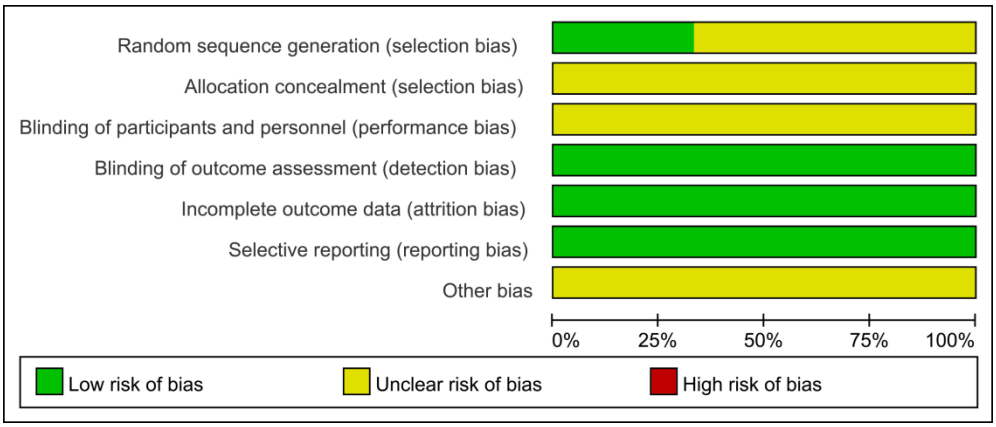

Fig. 3: The evaluation results of bias risk of inclusion study

Analysis of glycosylated hemoglobin

Four literatures [12, 14, 17, 18] reported the effects of SLBZS combined with western medicine on glycosylated hemoglobin, including 197 cases in the treatment group and 197 cases in the control group. Heterogeneity test showed that heterogeneity was not significant [$\chi 2=4.51$, df=3, P=0.21, I2=33%], and the fixed effect model was adopted. Meta-analysis showed that the

glycosylated hemoglobin in the treatment group was lower than that in the control group, and the difference was statistically significant [SMD=-0.47, 95% CI(-0.67,-0.26), Z=4.54, P<0.00001], as shown in fig. 4.

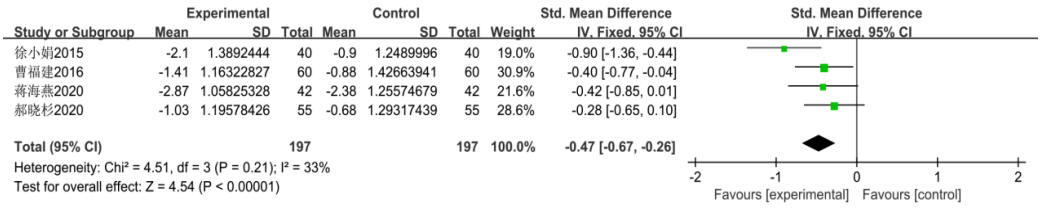

Fig. 4: The forest plot comparing of glycosylated hemoglobin of 2 groups of patients (Note: 徐小娟-Xu Xiaojuan, 曹福建-Cao Fujian, 蒋海燕-Jiang Haiyan, 郝晓杉-Hao Xiaoshan)

Analysis of 2h postprandial blood glucose

Six literatures [14-19] reported the effects of SLBZS combined with western medicine on 2h postprandial blood glucose, including 258 cases in the treatment group and 255 cases in the control group. Heterogeneity test showed that heterogeneity was not significant [χ 2 = 3.82, DF = 5, P = 0.58, I2 = 0%], and the fixed effect model was adopted. Meta-analysis showed that the 2h postprandial blood glucose in the treatment group was lower than that in the control group, and the difference was statistically significant [SMD =-0.73, 95% CI (-0.91,-0.55), z = 8.00, P<0.00001], as shown in fig. 5.

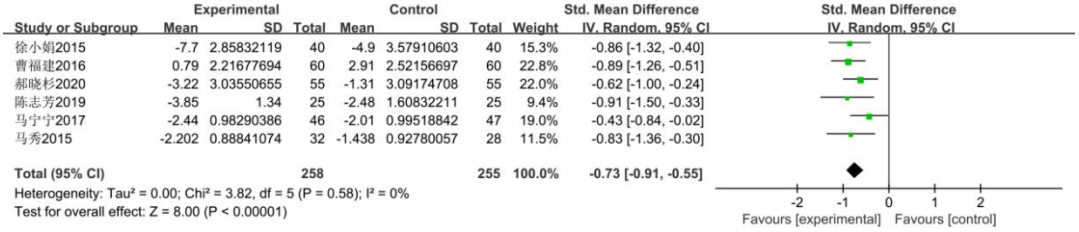

Fig. 5: The forest plot comparing of 2h postprandial blood glucose of 2 groups of patients, (Note: 徐小娟-Xu Xiaojuan,曹福建-Cao Fujian, 郝晓杉-Hao Xiaoshan, 陈志芳-Chen Zhifang, 马宁宁-Ma Ningning, 马秀-Ma Xiu)

Analysis of fasting blood glucose

Six literatures [14-19] reported the effects of SLBZS combined with western medicine on fasting blood glucose, including 258 cases in the treatment group and 255 cases in the control group. Heterogeneity test showed that heterogeneity was significant [χ2=16, df=5, P=0.007, I2=69%], and the random effect model was adopted. Meta-analysis showed that the fasting blood glucose in the treatment group was lower than that in the control group, and the difference was statistically significant [SMD=-0.55, 95% CI(-0.87,-0.22), Z=3.31, P= 0.0009], as shown in fig. 6.

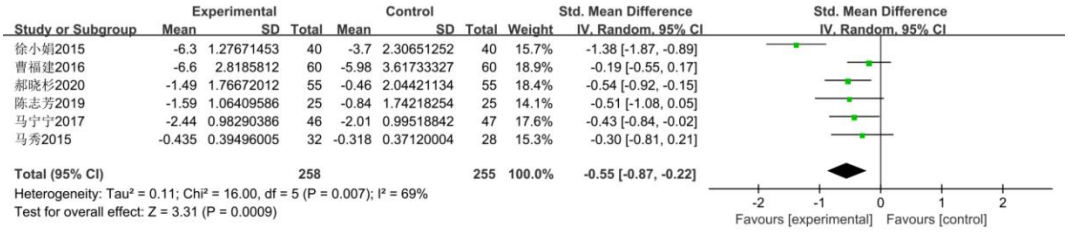

Fig. 6: The forest plot comparing of fasting blood glucose of 2 groups of patients, (Note: 徐小娟-Xu Xiaojuan, 曹福建-Cao Fujian, 郝晓杉-Hao Xiaoshan, 陈志芳-Chen Zhifang, 马宁宁-Ma Ningning, 马秀-Ma Xiu)

Analysis of homa-IR

Two literatures [13, 16] reported the effect of SLBZS combined with western medicine on Homa-IR, including 89 cases in the treatment group and 90 cases in the control group. Heterogeneity test showed that heterogeneity was not significant [χ2=1.02, df=1, P=0.31, I2=2%], and the fixed effect model was adopted. Meta-analysis showed that Homa-IR of patients in the treatment group was lower than that in control group, and the difference was statistically significant [SMD=-1.05, 95% CI(-1.37,-0.74), Z=6.58, P<0.00001], as shown in fig. 7.

Analysis of waist-hip ratio

Two literatures [17, 18] reported the effect of SLBZS combined with western medicine on waist-hip ratio, including 100 cases in the treatment group and 100 cases in the control group. Heterogeneity test showed that heterogeneity was not significant [χ2=0.52, df=1, P=0.47, I2=0%], and the fixed effect model was adopted. Meta-analysis showed that Homa-IR of patients in the treatment group was lower than that in control group, and the difference was statistically significant [MD=-0.17, 95% CI(-0.24,-0.1), Z=5, P<0.00001], as shown in fig. 8.

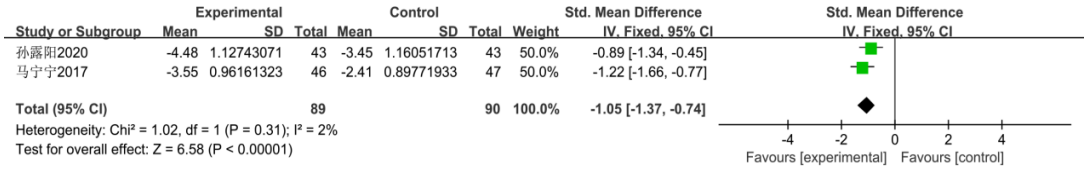

Fig. 7: The forest plot comparing of Homa-IR of 2 groups of patients, (Note: 孙露阳-Sun Luyang, 马宁宁-Ma Ningning)

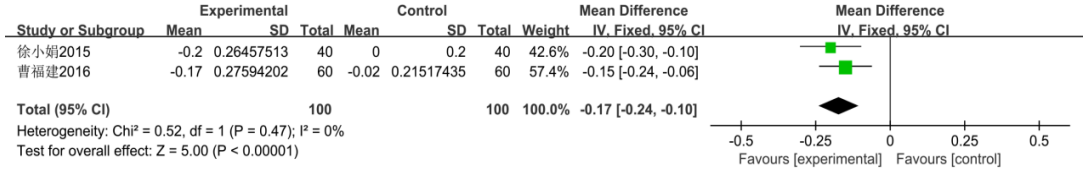

Fig. 8: The forest plot comparing of waist-hip ratio of 2 groups of patients (Note: 徐小娟-Xu Xiaojuan, 曹福建-Cao Fujian)

Analysis of BMI

Four literatures [11, 17-19] reported the effects of SLBZS combined with western medicine on BMI, including 175 cases in the treatment group and 171 cases in the control group. Heterogeneity test showed that heterogeneity was not significant [χ2=3.94, df=3, P=0.27, I2=24%], and the fixed effect model was adopted. Meta-analysis showed that the BMI of patients in the treatment group was lower than that in the control group, and the difference was statistically significant [MD=-0.68, 95% CI(-1.05,-0.31), Z=3.58, P= 0.0003], as shown in fig. 9.

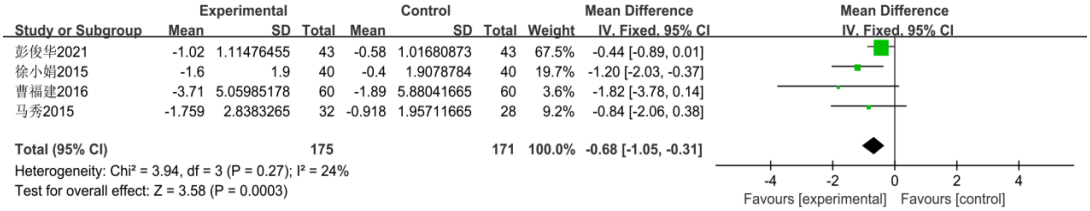

Fig. 9: The forest plot comparing of BMI of 2 groups of patients, (Note: 彭俊华-Peng Junhua, 徐小娟-Xu Xiaojuan, 曹福建-Cao Fujian, 马秀-Ma Xiu)

Analysis of GLP-1

Two literatures [11, 16] reported the effect of SLBZS combined with western medicine on GLP-1, including 89 cases in the treatment group and 90 cases in the control group. Heterogeneity test showed that heterogeneity was not significant [χ2=0.62, df=1, P=0.43, I2=0%], and the fixed effect model was adopted. Meta-analysis showed that GLP-1 in the treatment group was higher than that in the control group, and the difference was statistically significant [MD = 5.08,95% ci (4.62,5.54), Z=21.54, P<0.00001], as shown in fig. 10.

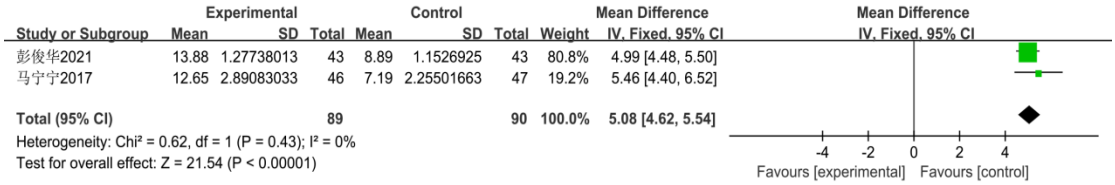

Fig. 10: The forest plot comparing of GLP-1 of 2 groups of patients, (Note: 彭俊华-Peng Junhua, 马宁-Ma Ning)

Results of Network Pharmacology

Related targets of diabetic obesity

A total of 337 genes related to diabetic obesity were downloaded from GEO chip, as shown in table 2.

Action target of SLBZS on diabetic obesity

A total of 2067 targets of Shenling Baizhu San (SLBZS) were obtained from TCMSP, TCMID and BATMAN-TCM. See table 3 for details. Then, the Venny diagram was drawn to obtain the intersection of the target genes of diabetic obesity gene and SLBZS, namely, the target of Shen Ling Baizhu San acting on diabetic obesity, as shown in fig. 11. In addition, there were 59 intersection targets, as shown in table 4.

Analysis of the core targets of SLBZS powder on diabetic obesity

The above 59 targets were input into String platform (https://www.string-db.org/) for protein interaction analysis, and the network diagram of protein interaction was obtained, as shown in fig. 12. Then, the network diagram was input into Cytoscape_v3.8.2, and three core targets of SLBZS on diabetic obesity were screened, as shown in fig. 13.

Table 2: Related targets of diabetic obesity

GSE	GENE	GSE	GENE	GSE	GENE	GSE	GENE	GSE	GENE
GSE73034	DIP2C	GSE64998	AEN	GSE42902	WASHC3	GSE42902	GLA	GSE42902	PNRC2
GSE73034	HEXIM1	GSE64998	AHCY	GSE42902	XRCC2	GSE42902	GLYAT	GSE42902	PODXL
GSE73034	IZUMO4	GSE64998	AJUBA	GSE42902	ZEB1	GSE42902	GNS	GSE42902	POLR2L
GSE73034	EIF4EBP1	GSE64998	AKR1A1	GSE42902	ZFP69B	GSE42902	GPR137B	GSE42902	POPDC3
GSE73034	GIPC1	GSE64998	ALPK2	GSE42902	ZNF146	GSE42902	GSTO1	GSE42902	PPFIBP2
GSE73034	FXYD3	GSE64998	ARRDC4	GSE42902	ACLY	GSE42902	GSTT1	GSE42902	PRCP
GSE73034	CFTR	GSE64998	ATG2B	GSE42902	ACSS2	GSE42902	HDGFL3	GSE42902	PRKG1
GSE73034	LHPP	GSE64998	C11orf1	GSE42902	ADAMDEC1	GSE42902	HHEX	GSE42902	PTER
GSE73034	ANKHD1-EIF4EBP3	GSE64998	C12orf49	GSE42902	ADAP2	GSE42902	HIST1H3E	GSE42902	PTGER2
GSE73034	IZUMO4	GSE64998	C5orf24	GSE42902	ALCAM	GSE42902	HLA-DPA1	GSE42902	PTGR2
GSE73034	C1ORF63	GSE64998	CA14	GSE42902	ALDH1B1	GSE42902	HLA-DPB1	GSE42902	RAPGEF5
GSE73034	GRB14	GSE64998	CDKN1A	GSE42902	AOC3	GSE42902	HSPH1	GSE42902	RFWD3
GSE73034	LRRC23	GSE64998	CDNF	GSE42902	AP2M1	GSE42902	HTATIP2	GSE42902	RGS17
GSE73034	DBNDD1	GSE64998	CRELD2	GSE42902	APOE	GSE42902	IFITM2	GSE42902	RNF139
GSE73034	HOMER	GSE64998	CSTB	GSE42902	ARL14EP	GSE42902	IGF1	GSE42902	RNF212
GSE73034	FAM43B	GSE64998	ENPP3	GSE42902	ASS1	GSE42902	IL7R	GSE42902	RORB
GSE73034	C1ORF135	GSE64998	FAM53B	GSE42902	ATP23	GSE42902	JAM2	GSE42902	RRM2
GSE73034	TOMM40	GSE64998	FAT1	GSE42902	ATP5IF1	GSE42902	KCNA1	GSE42902	RUNX2
GSE73034	KIAA1109	GSE64998	GAS6	GSE42902	ATP6V1C1	GSE42902	KCNN2	GSE42902	S100A1
GSE73034	EPPK1	GSE64998	GNA12	GSE42902	AZGP1	GSE42902	KIAA1147	GSE42902	S100A8
GSE73034	PHKB	GSE64998	GOLM1	GSE42902	BCL10	GSE42902	KIRREL3-AS3	GSE42902	S100B
GSE73034	FAM168A	GSE64998	GPC1	GSE42902	BGN	GSE42902	KLHL31	GSE42902	SAMSN1
GSE73034	C9ORF103	GSE64998	H2AFY2	GSE42902	BIRC5	GSE42902	KLHL6	GSE42902	SCD
GSE73034	BAG2	GSE64998	HBB	GSE42902	BNIP2	GSE42902	KYNU	GSE42902	SERPINB7
GSE73034	BEX2	GSE64998	HNMT	GSE42902	C3AR1	GSE42902	L3MBTL4	GSE42902	SERPING1
GSE73034	HAUS4	GSE64998	HPS5	GSE42902	C9orf78	GSE42902	LBH	GSE42902	SESN2
GSE73034	C20ORF132	GSE64998	HYOU1	GSE42902	CA3	GSE42902	LCP1	GSE42902	SFT2D1
GSE73034	LAMB2	GSE64998	IKBKG	GSE42902	CCDC102B	GSE42902	LINC00189	GSE42902	SLAMF1
GSE73034	TAL2	GSE64998	IL32	GSE42902	CCDC15	GSE42902	LINC00339	GSE42902	SLC11A2
GSE73034	GTF2H4	GSE64998	KLF12	GSE42902	CCNB2	GSE42902	LINC00471	GSE42902	SLC25A1
GSE73034	BPGM	GSE64998	KMO	GSE42902	CDC45	GSE42902	LINC01121	GSE42902	SLC25A37
GSE73034	TET1	GSE64998	KYNU	GSE42902	CDC6	GSE42902	LOC554206	GSE42902	SLC44A2
GSE73034	GFER	GSE64998	L3MBTL3	GSE42902	CDH13	GSE42902	LPCAT3	GSE42902	SLC50A1
GSE73034	SYM	GSE64998	LOC100419773	GSE42902	CDKN2B	GSE42902	LRCH1	GSE42902	SNX10
GSE73034	CHRNA7	GSE64998	MTUS1	GSE42902	CENPU	GSE42902	LRRC4C	GSE42902	SPARC
GSE73034	EPHX2	GSE64998	NAPEPLD	GSE42902	CKB	GSE42902	LYZ	GSE42902	SPINK1
GSE73034	POLR3D	GSE64998	NR5A2	GSE42902	CKS2	GSE42902	MBOAT2	GSE42902	SPP1
GSE73034	LINC00310	GSE64998	NUDT13	GSE42902	CLEC7A	GSE42902	MCM10	GSE42902	SPTAN1
GSE73034	NUCB2	GSE64998	NUDT9P1	GSE42902	CLHC1	GSE42902	MCM6	GSE42902	SPX
GSE73034	KCTD15	GSE64998	OR3A1	GSE42902	CLSPN	GSE42902	ME1	GSE42902	SRGN
GSE73034	RELB	GSE64998	PAIP2B	GSE42902	CRYZ	GSE42902	MMAB	GSE42902	SRSF10
GSE73034	LYG2	GSE64998	PELI2	GSE42902	CTSA	GSE42902	MYO1E	GSE42902	ST6GALNAC2
GSE73034	ADAM17	GSE64998	PIGR	GSE42902	CTSB	GSE42902	NARF	GSE42902	SWAP70
GSE73034	LANB1	GSE64998	PPIL1	GSE42902	CYC1	GSE42902	NCAPG	GSE42902	SYTL4
GSE73034	CEMIP	GSE64998	PPIP5K1	GSE42902	CYLD	GSE42902	NDRG3	GSE42902	TAB2
GSE73034	KLHL18	GSE64998	PPM1K	GSE42902	DDX43	GSE42902	NDUFA6	GSE42902	TACSTD2
GSE73034	MAP6	GSE64998	PSD3	GSE42902	DGAT2	GSE42902	NETO2	GSE42902	THBS1
GSE73034	LRRC3C	GSE64998	PYY	GSE42902	DHCR24	GSE42902	NFATC2	GSE42902	THRSP
GSE73034	ALG11	GSE64998	RBMS1	GSE42902	DHCR7	GSE42902	NOVA1	GSE42902	TLL1
GSE73034	FAM86DP	GSE64998	RBMS1	GSE42902	DHRS7	GSE42902	NTAN1	GSE42902	TMEM47
GSE73034	CCDC36	GSE64998	RET	GSE42902	DNAJB4	GSE42902	NTPCR	GSE42902	TMEM97
GSE73034	CREBB	GSE64998	RFX5	GSE42902	DNAJB9	GSE42902	NTRK3	GSE42902	TNFAIP3
GSE73034	KRT79	GSE64998	SEPSECS	GSE42902	DPY30	GSE42902	OR13A1	GSE42902	TNFRSF10D
GSE73034	CTP1	GSE64998	SERPINE1	GSE42902	DTL	GSE42902	OTUD6A	GSE42902	TNFRSF11B
GSE73034	KIAA0930	GSE64998	SGCB	GSE42902	EBP	GSE42902	PAPD5	GSE42902	TNMD
GSE73034	CD1C	GSE64998	SLC16A12	GSE42902	EGFL6	GSE42902	PAX8-AS1	GSE42902	TP53I3
GSE73034	COPS5	GSE64998	SMPDL3A	GSE42902	ELP5	GSE42902	PBX3	GSE42902	TPRG1
GSE73034	SLC16A10	GSE64998	SNORD63	GSE42902	FADS1	GSE42902	PCLAF	GSE42902	TRGV7
GSE73034	WIPF2	GSE64998	SULF2	GSE42902	FADS2	GSE42902	PCOLCE2	GSE42902	TRIM36
GSE73034	RCBTB1	GSE64998	TES	GSE42902	FAM111B	GSE42902	PCYT2	GSE42902	TSPAN6
GSE73034	CRADD	GSE64998	TNRC6C	GSE42902	FAM118A	GSE42902	PDGFRL	GSE42902	TTC12
GSE73034	ARHGEF16	GSE64998	VAMP8	GSE42902	FAM92A	GSE42902	PEX11B	GSE42902	TTTY12
GSE73034	HEXIM1	GSE64998	VRK2	GSE42902	FASN	GSE42902	PGM2L1	GSE42902	TYMS
GSE73034	ZNF300	GSE64998	WBP1L	GSE42902	FTL	GSE42902	PLA2G7	GSE42902	UBE2B
GSE73034	DZIP3	GSE42902	AACS	GSE42902	FYB1	GSE42902	PLK4	GSE42902	UCHL1
GSE73034	AGL	GSE42902	ABCC3	GSE42902	GINS2	GSE42902	PMVK		
GSE64998	ZNF577	GSE42902	ABHD15	GSE42902	ZNF223	GSE42902	ZNF510		
GSE64998	AASS	GSE42902	ACACA	GSE42902	ZNF285	GSE42902	ZNF521		
GSE64998	ACADSB	GSE42902	ACAT2	GSE42902	ZNF439	GSE42902	VIP		

Table 3: Targets of SLBZS from TCMSP

Targets of SLBZS from TCMSP										
P3H3	UROD	HCN4	LHX6	XDH	JUNB	TSC22D1	TICRR	PTMA	ELANE	MAP2K1
PARS2	SLC38A7	NCKAP1L	P2RY1	GFER	MEX3C	NOS2	HPRT1	UBE2I	SIGMAR1	GNA15
P4HA1	PF4	EIF2AK1	MAOA	APRT	ABCA1	BHMT	INHBA	BCL2	CTSG	ARFGEF2
PYCRL	MYO5A	PRSS12	GATA3	TOX3	ABHD5	NOS3	ADCY8	RBFOX2	NCF4	P2RX1
PPIB	NPPA	FGFR2	P2RY2	SRC	ALOX15	DYNLL1	DGAT2	RNF4	NCF2	LRP2
P4HB	ARHGEF2	IL1RN	ACTN4	WNT5A	PAWR	APIP	SLC2A1	FKBP5	GAA	PTGS1
SLC7A4	HSD17B8	IFNG	PALM	TGFB1	FABP3	SUPV3L1	KCNJ8	ARNT	MGAM	IGHG1
PPIAL4F	RYR2	ROCK2	DNMT3A	UBR5	CYR61	GUCY1A2	GBA2	TRIP4	GANAB	CALM
RARS	GJA5	ROCK1	MC3R	TFAP2C	RRM2	TMEM27	WRB	ETFB	GANC	LYZ
NOXRED1	GNAS	BMP4	PIK3R3	SERPINB3	PYGL	ACE	APLP1	CCNE1	KCNJ1	VEGFA
DAZAP1	SULT2A1	AGRN	GPM6B	AREG	PRKAB2	NOS1AP	SPIDR	MED23	KCNJ12	MMP2
PARK7	SCN11A	PDE2A	DTNBP1	PDGFB	ACVR1	SLCO1B3	KCNJ11	MDM2	KCNJ10	MMP1
STOM	SCN3B	PDE3A	HAND2	TNFSF11	ASNS	SLCO1B1	NR2F2	MTA3	KCNJ15	CASP7
YTHDC2	SCN3A	GABRB2	CAV2	LEF1	MAT1A	PLA2G2E	HK1	FLII	KCNJ14	F3
PPIG	ALDH5A1	GABRA5	IL13	PHB	ASS1	AKR1C4	SLC28A1	GTF2B	GGT1	GJA1
PPIA	COX7A1	GABRG2	ANXA7	GPER1	NAE1	KCNQ3	VIM	CDK2	GLO1	MMP10
PPIH	COX6A2	RXRA	LRTOMT	ITFG2	MUT	TPMT	PRPS2	CUEDC2	GPX6	ADH1A
P3H2	COX6B1	SEMA4D	CRHR2	DGUOK	CUBN	KCNQ2	CD276	PIAS2	GSTT1	PRSS3
TWIST1	COX7B	MIF	HTR7	SLC5A6	MMAA	MPO	NIT2	LDB1	GSTM3	PLAU
SLC7A2	COX8A	FASLG	SLC9A3R1	MCCC1	XBP1	AKR1C1	IRAK1	MED13	GPX2	LPL
PPIAL4D	SUCLG1	CRP	PIK3R1	MDH2	RALA	CHUK	ZFPM1	CEBPB	MGST2	PON1
AIMP1	TMLHE	IL1B	ARX	YBX1	ASNSD1	IKBKE	AQP9	MED14	GSTZ1	ENPEP
RHOA	BBOX1	SLC44A4	VIP	CSNK2B	BICD1	DHDH	RPS3	SMARCA4	GSTA4	NTRK2
ALKBH7	SDHC	ANGPT1	CRHR1	GALNT6	RRM2B	GLTP	GRK5	POU4F2	MGST1	DNPEP
MLXIPL	SDHD	PLN	CABP1	HSPA1L	POLE2	PRKACA	VHLL	DNTTIP2	LTC4S	PGF
SYNCRIP	SLIT2	HRC	FLOT1	ARHGAP29	POLE4	USP7	NAGS	NCOA4	GSTA3	DPP4
OAT	SLC1A3	ADIRF	ACVR2A	HSPD1	ASNA1	MGMT	MGEA5	HBA2	HAGH	NR3C2
VAPB	UROS	FNTA	SRI	AKR1B10	AMHR2	PRKDC	LCAT	MED12	MGST3	CA2
ALDH4A1	TOP1	AHCY	GPR39	WRN	ABL2	UHRF2	SERPINA7	PAK6	GSS	ORF21
PPIC	GRIN2D	IKBKB	ARRDC3	PCCA	ABCC9	HELLS	ADAM17	PPARGC1A	GSTO2	PRSS3
SLC6A14	SRD5A1	CHDH	SLC22A3	MCCC2	MAT2A	UHRF1	ADCY2	ITGB3BP	GPX8	TOP2
PYCR2	ACSS2	HCN2	RXRB	ILK	APAF1	KDM1A	NMNAT3	ZBTB17	GPX5	TRYP1
SLC6A7	SIX4	GABRB1	RARA	CIAO1	MMAB	POLD1	SCARB1	MED20	GSTK1	GSK3B
CRTAP	CCL2	GABRA3	RARRES1	LAMA3	AMN	DNMT3B	BMPR1A	NELFB	HPGDS	PKIA
SLC7A3	ANK2	GABRA6	GPRC5A	CSNK2A2	SMAD3	POLG	SLC27A1	EP300	GSTA1	blaC
PPIAL4E	TH	PDE3B	NR0B1	PRKAA1	FBP2	PAX5	AKT3	SLC30A9	GPX4	CCNA2
ACTN3	DHODH	HMGA2	RARB	USP9Y	ABCG4	CTCF	ACSS3	MPG	GSTA5	SELE
HOGA1	GALC	NRG1	RARG	ELL3	POLE	LIG4	SMAD4	CHD9	GPX3	JAK2
PRPF4	CYP39A1	DMGDH	RXRG	CHGB	CREB1	TRDMT1	SMAD5	PSMB9	GLRX	KDR
DDX3X	STIM1	LGALS3	ALDH1A2	ACACB	HINT1	KDM3A	INHA	ESRRA	GSTM1	CHEK1
SNRPA	DHTKD1	TLR3	PPP2CB	HLCS	RRM1	PLA2G2A	FGF1	NCOA7	GPX1	MAPK10
OGFOD1	KCNE5	SHH	SEC14L3	NAT10	ADRBK2	ITGB2	GET4	RBM23	GSTP1	AMY2A
EGLN1	UGT8	ADORA2B	SEC14L2	GOT1	TNK2	ITGAL	BMPR1B	CCNT1	ESD	AKR1B1
RPL13A	ACSS1	AURKA	PPP2CA	DIAPH3	GNMT	CYP19A1	EFNA1	TRAM1	GSTM2	LTA4H
PYCR1	CRACR2A	DNM3	DGKA	MCF2L2	ABL1	MTAP	BMPR2	RLIM	GSTM5	ATP5F1B
PPIF	ILVBL	TGFB2	PTGS1	ATXN1	AMD1	PRPS1	HUS1B	UNC119	GSTA2	MT-ND6
L3HYPDH	OGDHL	CDH8	PRKCA	CSNK2A1	ABCC8	Spermidine	OXSM	PRPF6	GSTM4	MAPK8
P4HA2	ACADM	HPN	PRKCB	PC	ARAF	B4GALT2	IRS2	POLR2D	GSTO1	CRK2
EARS2	CTNNB1	APOA1	NR1I2	PCCB	MTRR	DEFB126	PKD1L1	TNFRSF14	GLRX2	FASN
KARS	HAP1	IDO1	SEC14L4	BRCA1	MMACHC	RENBP	AMH	ERBB2	TXNDC12	LDLR
PPIAL4A	DHRS9	SOX9	POLA1	HIST2H2AB	ATF4	NAGLU	SREBF1	MNAT1		ABCC1
GOT2	SLC25A13	GABRG3	PCNA	HSPA5	VLDLR	NAGPA	SLC16A2	POU2F1	PDE7A	BACE1
SART3	NFX1	GABRG1	SOAT1	PRKAA2	POLE3	NAGK	TYMP	YWHAH	PDE7B	RB1
EGLN2	SCN2B	GABRA1	MTTP	CHCHD2	ACSL1	B4GALT4	TCAF2	C14orf1	PDE4C	CDK4
SNRPB2	COX6C	PDE4D	SOAT2	DYNC1H1	CBS	B4GALT3	FBXO18	GADD45A	CES2	MMP3
BAX	AKR1C2	CD74	CNR2	CMYA5	AFG3L2	GNE	MAP3K14	TRRAP	NMUR2	EGF
DNAJC15	SCN2A	NKX3-1	VDR	ACACA	ACVR1B	BLVRB	IGSF1	BDNF	CES5A	SULT1E1
P4HA3	FECH	KLF4	SNAI2	MCC	ALK	FLAD1	PLIN5	FOXO3	PTGDR	THBD
PRODH	SCN9A	RIPK1	FGF23	MYC	SLC25A4	RPL31	MME	NR4A1	ALAD	COL3A1
EPRS	FABP6	ALDH7A1	S100G	SNX27	MTR	PROZ	S1PR3	PTPN6	LIPA	GYRB
PROSC	SCN1B	WNT2	CYP27B1	KPNA3	SLC25A6	GGCX	CERS1	NR2F6	ANG	CTSD
P3H1	NR1H4	FCER2	NFKB1	KPNA2	UGCG	TXNRD3	THNSL2	PPP1CC	SLC7A7	APP
PRODH2	HSD17B6	RAPGEF2	MED1	DDX52	CASP9	VCP	TPM1	GADD45B	ATCAY	MET
SLC7A1	PLOD1	ASCL1	GFI1	CHRM1	UBA3	RFK	CD24	MED24	SIRT4	CTRB1
PPIAL4C	SDHB	NCOA1	KL	CHRM5	ADCY1	ORM1	SMURF2	KIF1A	IREB2	ADCYAP1
GAPDH	ACO2	KMT2A	CYP27A1	SI	PIM1	SLC19A2	PYGM	FHIT	PAX8	SAA1
CPEB3	SALL1	CAMK2G	TRIM24	CHRM4	AKT1	BGLAP	ADCY6	BCAS2	ACO1	npr
ALDH18A1	SLC13A5	ADORA2A	GC	CHRNA10	ACVRL1	VKORC1L1	NUDT1	CPT1A	FGF19	PLA2G4A
VAPA	CACNA1A	GRIA2	SNAI1	GP9	DCK	ACP5	SOX4	CALM1	CES3	
TBC1D20	PLG	ADA	LANCL2	CHRNB3	CBSL	FOLR2	UBL4A	MVP	MTNR1A	
EGLN3	ADORA1	FURIN	CYP2R1	KCNN4	CDK15	ATP4A	GBA	FAM45A	HPCA	

Targets of SLBZS from TCMSP								
SNCA	FBXO45	HOMER1	KANK2	CHRNE	ABCB11	F7	ASL	ISL1	PDZD3
CXCR4	ARV1	PIK3CG	SNW1	KCNK6	TCN1	F10	LGALS9	PRDM2	NPY2R
ACHE	MRPS36	KCNB1	CYP24A1	CHRNA5	SLC25A5	TPK1	ABCA12	KMT2D	GPR50
DRD2	BCKDK	NPY5R	CYP3A4	CHRNG	SAXO1	F2	PPP4C	TRIM28	GPR27
CHRNA2	HSD17B2	ANK3	PML	CHRND	TGFBR2	FOLR3	SOX17	CDK8	CD36
SLC18A2	EPO	AVPR2	IRX5	CHRNB4	JAG1	RAB1A	BAK1	REXO4	SDC4
HTR3A	CLN3	RYR3	GPBAR1	KCNK1	ABCA7	AGTR1	PROX1	MTA2	CD47
BCHE	PLCG2	GRIK5	CALB1	CHRNA1	GRB2	BLVRA	UCHL1	WIPI1	SOD3
CHRM2	BCKDHA	GRIK1	TCF3	CHRNB1	44263	DNAJB9	SLX4	KBTBD7	TP53I3
CHRM3	GAL3ST1	GRM7	B4GALT1	TRPV3	PDGFRB	PROS1	PPAP2B	PNRC2	CYP4F11
PDE5A	NEDD4L	ADORA3	KCND1	TRPM8	DDR2	F9	ADIPOR2	PELP1	SOD2
PDE11A	SRD5A3	CHRNA9	GAMT	TRPA1	NRP1	PROC	PTPN22	HTR6	CRYZL1
ALOX5	ETHE1	CDK5R2	CAT	F12	NTRK1	SLC52A3	APOC3	STRN	CBR4
SERPINE1	CYP4B1	UTS2	KCNC1	CRYZ	DDR1	NPR1	NOTCH4	AHR	SOD1
COMT	HSD17B1	SHANK3	KCND2	VKORC1	PDGFRL	RPL3	RASGRP1	POU2F2	UBIAD1
ESR1	CAV3	CETN2	KCND3	FFAR1	SORT1	RPL3L	ASRGL1	GRIP1	CCS
AKR1D1	KCNA5	KCNA1	RDH13	FADS1	CSF1R	SLC25A32	RIPK3	RPS6KA1	CETP
ABAT	SQRDL	ADRBK1	ALDH1A3	CKMT2	PDGFRA	ACPP	ABCB4	TSC2	APOH
COX5B	ETFDH	GHRL	NFIB	ACSL3	CSF1	SLC23A1	CAD	SAFB	PIK3CA
SCN7A	PCSK9	UTS2R	NRXN1	SLC9A1	ZEB2	TKTL1	ATP2B4	NCOA6	PIK3CB
COX5A	GPR143	CRH	SOX15	LPCAT1	KIT	THTPA	MUS81	NRIP1	ITPR3
COX4I1	SFXN5	SPX	GPX7	NDRG2	EPOR	SLC26A6	RLTPR	RBBP5	ATM
SCN4A	DBT	GRIK4	NKX2-1	HOPX	MST1R	SLC23A2	BAG6	YWHAQ	G6PD
CES1	HTR2A	KDM6B	RNASE2	NR1H3	NFKB2	CERS2	GDPGP1	SMARCD1	ATP11C
COX2	HTR1D	FOS	KCNA3	FMR1	MMP9	SLC35F3	GRK6	SMARCA2	ADAP2
SUCLG2	CALY	GRIK2	KCNC3	ITGB3	SMS	FOLR1	HBA1	TAP1	XCL1
SLC25A10	CHRNA4	TACR2	ALDH2	ANXA13	ALPPL2	SLC46A1	CREBBP	JUND	CASQ1
SUCNR1	CHRNA6	GRIA4	GUCY1B3	STX3	PIPOX	SLC19A1	RELA	NR2F1	IGF2
OXCT1	HTR2B	NAV2	RDH11	CAPN3	SMOX	C2orf83	VAV3	TADA3	SPR
SDHA	DRD3	GRIA1	DHRS3	GDF5	SAT2	SLC19A3	PRMT2	NR2C1	SELP
DCT	CHRNA7	TBR1	RDH12	PPARGC1B	ODC1	PRKAG2	PIAS1	TAF10	TAS1R3
JMJD6	CHRFAM7A	HMGCR	RLBP1	ELOVL6	AZIN2	PRKAG3	USF1	CRIPAK	CD63
HSD17B11	ADRA2A	ADCY3	CYGB	AVP	AZIN1	NCOR1	PTEN	ATAD2	RAG2
GRIN3B	DRD4	ATP2A1	IGF1	ZNF536	PAOX	CDKN2A	NSD1	FOXO1	PIK3CD
CACNA1B	DRD5	PARK2	EDN1	ALOX15B	AGMAT	GATA4	CITED1	TRIM25	ITPR2
GRIN3A	HRH3	KISS1	CNTNAP4	COL1A1	DHPS	SUPT20H	PDLIM1	FKBP1A	POLA2
GRIN1	HTR1B	EPHX2	SPARC	NOTCH1	SAT1	HNRNPK	ARHGEF15	PTGFR	PDE6B
SIRT1	HTR1A	GRIK3	CRLF1	NAPRT	PLD1	GCG	FHL2	LTK	PDE8A
SIX1	DRD1	KHDRBS1	ALDH1B1	NODAL	PLD2	CDK5RAP3	GADD45G	CAMK2A	GNAT1
OSBPL8	CHRNA3	CETN1	DARS	CCM2L	NAPEPLD	EDNRA	BCAR1	PDXK	XRCC4
UBE2B	HTR2C	AGT	MIP	CKM	PCYT1A	FOXP3	HNF4A	AOX1	GNAT3
STIM2	ADRA2C	SORCS3	STX1A	CKB	FSCN1	KAT2A	PRMT1	PNPO	NUDT9
COLGALT1	ADRA2B	CDK5R1	NRXN2	COL27A1	PCYT1B	CAV1	MAPK3	PDXP	CXCL13
ARID1A	HRH1	INS	DAB2IP	NAMPT	PLD4	RFWD3	RFX4	TKT	PTK2B
ACOT4	ADRB1	ATP1A2	PRKAB1	LARP4B	PLD3	NFKBIA	MTA1	IMPA1	LRRC8A
SLC25A12	OPRM1	SMO	ADH1B	ELOVL3	PHOSPHO1	PRKAG1	MED21	TPI1	C5
CDH11	PDE6G	GRIA3	KCNB2	METRNL	RAP1GAP	RPS6KA3	SAFB2	GPI	TET1
BDKRB2	KCNK2	NCBP2	KCNA4	FOXA1	KLF5	MAPK14	MED16	PSAT1	MTOR
SMAD7	CACNB4	CX3CR1	GATM	SLC8A2	PODXL	SREBF2	SMAD2	APOC2	ZFP42
WNT10B	CACNB2	FBP1	RBP3	ABCF1	ATP8B1	TP53	EIF3I	MAP2	FKBP1B
STAR	COLQ	DGKI	RDH5	ITGAV	HMOX1	PSME3	NCOA3	MAPT	HPS4
CAMK2D	CD34	ARPIN	RDH14	PTPN2	GPLD1	KAT2B	CRMP1	MAP4	XRCC6BP1
HTT	CACNB1	CHRNB2	NRXN3	PAX2	NPR3	WDR5	RBM39	EOMES	PDE1A
TST	CACNA1F	SLC18A3	RNASE4	NR1H2	NPR2	DHFR	COPS5	TBXAS1	NT5E
TMEM110	ADRA1D	ATP13A2	LEP	AGTR2	HTR3B	INSR	GNAI1	IL2	IDNK
EPHA4	CACNB3	LRRK2	PAXBP1	ANAPC2	CACNG1	GAS6	MED6	PLA2G2D	NT5C1A
EDA	PDE6H	CALCA	CYP2E1	CDC20	DMTN	HSP90AB1	EIF6	PFKL	PPP3CB
KCNQ1	CNR1	PCSK6	ADH1A	NR1D1	MTNR1B	ATIC	SOS1	IL17RA	HELB
UGT1A1	CACNA1C	PPP3R2	KCNA2	ELOVL7	AOC3	RAB8B	PHB2	SLC7A11	FER
PLOD2	KCNH2	NOX1	DLG4	WDR77	RNF207	PARP10	NPDC1	HCAR2	BCL11B
SLC25A1	ADRA1A	ATP1B1	KCNA7	GJD4	EPHB1	PDE10A	NCOA2	TBX21	HIBADH
TYR	OPRD1	ALDH1A1	KCNK4	CPLX2	VCAM1	PDE9A	BAG1	F2RL1	C2CD5
SCN1A	CACNA1S	S100A9	RETSAT	SLC35G1	SLC29A1	HOXA5	PTGES3	LTF	MMP28
COX7C	ADRA1B	NR3C1	DHRS4	FGF2	ADAM8	CMPK2	CDK7	ALDOB	PIK3R6
SCN5A	SLC17A7	CYP17A1	RDH8	SLC8A1	KCNMA1	HYAL2	RNF14	ALDOA	RAG1
COX3	WLS	HSD11B1	LRRC4B	TRPV1	P2RX2	TBPL1	TCF20	ALDOC	TNFAIP3
HDAC9	RAB7A	CREBRF	ACY3	SLC6A8	CACNG2	FBLN1	KAT5	CD28	TREM1
SCN4B	CALCOCO2	WNT4	MAGI2	CKMT1A	KCNJ9	NT5M	GTF2H1	CD40	LAMP2
ACADSB	ADRB2	FXYD2	RAB3A	ALDH3A1	SLC28A3	PDE1B	MKNK2	IL18R1	TAS1R2
OGDH	ARRB2	AKAP13	RNASE8	SERPINB7	CACNA1H	CDKN1A	BTF3	OCLN	ITPR1
SLC13A2	ESR2	ANXA1	SNTG2	PTGER2	ZP4	SLC22A6	CALM2	TICAM2	RINT1
SLC13A3	OPRK1	PRLR	NLGN1	RGCC	GLRB	DPYS	DDX5	BCL2L11	AMPD3
PLOD3	TUBD1	NR3C2	ZPR1	ELOVL1	MSN	DUT	NCOR2	CSF2	QDPR

Targets of SLBZS from TCMSP									
AKR1C3	TUBA4A	TSPO	PAX7	NUFIP2	GLI3	HIF1A	CDC25B	BAD	VTI1A
SLC13A4	TUBA3C	RAD51	ADH4	OXER1	AOC2	HSP90AA1	CLIC1	RIPK2	STAP1
TYRP1	TUBB3	ATP1A1	ACY1	CYP4F2	TNR	DTYMK	POU4F1	IL17A	HIPK2
CACNA2D1	TUBB6	CAMLG	KCNA10	ALDH8A1	EEA1	DHFRL1	LCK	MYD88	PPP3R1
CACNA2D2	SLC38A3	BMP2	TPO	SERPINH1	ICAM1	STUB1	DDX17	FUT7	PGLS
GRIN2C	TUBB	DKK3	KCNC2	GNAT2	GLRA2	PYGB	STAT5A	SULF2	CALHM1
HDAC1	TUBG1	BMP5	RNASE1	S100A8	KCNJ6	NTN1	BAZ1B	GSK3A	TAL1
SHMT1	TUBA1C	REST	KCNA6	SP1	HTR3D	ORMDL1	CCNH	PHKG2	RYR1
BDH1	EHHADH	NOTCH2	IYD	NEUROD2	KCNJ5	CD2	MED17	HTR1E	PDE6A
SPI1	TUBB8	PGR	RBP1	JAK3	SLC29A2	HK2	STAT3	SLCO2B1	PGD
CYP1A2	DAB2	ATP1A3	LRAT	WNT11	HTR3C	WHSC1	TDG	SULF1	PDE1C
PKD2	TUBE1	COL5A1	ADH7	DNAJA3	SLITRK6	VDAC3	FKBP4	RGS2	PDE6C
NEDD4	TUBA1A	SHBG	AQP8	SLC3A2	SUMO1	SLCO4A1	UBC	HTR1F	CTR9
PHGDH	TUBA1B	NR1I3	ASPA	MECOM	P2RX3	CCND1	SVIL	ARRB1	TAS1R1
YBX3	TUBA8	PDE8B	APOE	PPARA	GHRH	BLM	ZBTB16	PDGFA	MCM3
CACNA1D	TUBB2B	SLC6A3	MC4R	ABCG1	ZP3	DDIT3	PSMC5	HTR4	LONP1
PRPH	JUN	SLC18A1	KCNIP2	ELOVL4	POU4F3	HMBS	NR2C2	APLN	PPP3CA
PRDM8	TUBG2	CEND1	SCGB1A1	SC5D	CARTPT	SHTN1	CUL4B	EDN2	TALDO1
DLST	TUBA3D	MOXD1	PPARD	PTGER1	KCNJ3	MZB1	UBE3A	NGFR	ABCC4
AP3D1	TUBB4A	FEZF2	ALDH3B1	PTGER3	HTR3E	SLC16A10	HRH4	CBFA2T3	DPPA3
IL10	TUBB2A	FLNA	ALDH3B2	IHH	GLRA1	ORMDL2	HEXIM1	BNIP3	ADAP1
SLC1A6	TUBB1	SLC22A2	PADI4	FNDC5	FOXL2	SAMHD1	IGF1R	NEFH	AMICA1
CDC42	TUBB4B	OPRL1	GLRA3	MAPK9	AOC1	NKD1	PTPN1	AQP1	RTN2
OCA2	ABCB1	MAOB	TYMS	RPL7A	HCRT	PPID	ASH2L	NEFL	GLYR1
HACL1	TUBA3E	UCN	GCDH	PTGIS	EZR	MLLT3	HSPA4	TAC4	PIK3R5
CASQ2	PCK1	OXTR	POR	NPPC	SLC9A6	NMNAT1	TRIM59	TAC1	MC2R
DLD	PDE4A	CHP1	TXNRD1	MATN1	GLRA4	GFAP	MED10	UCN2	SCT
CYP1A1	GABRA2	RAB3B	AIFM1	ALOX5AP	PRKCD	PID1	RGS3	CDH3	PTPRO
SRD5A2	TNF	SHANK1	DNMT1	FGF4	CD300A	CPS1	POLR1B	CACNA1I	HRH2
ESRRG	GABRP	PTGS2	AK5	GNB2L1	CHGA	SLC27A5	FOXO4	DAPK2	TUSC2
COX1	GABRQ	SYT1	AK9	TBC1D32	APOC	NMNAT2	DDX54	CYP11B2	LAMP1
SCN10A	PDE4B	PINK1	NT5C2	RET	KIF14	ADIPOR1	SHC1	HPGD	EGR1
PLA2G1B	SLC6A2	AVPR1B	PNP	SCD	HSD17B7	HUS1	PIAS3	CACNA1G	PPP1R9B
ADH1C	APOA2	DBH	ERO1B	PLCB1	CRYM	TGFBR1	SMARCE1	CYP11B1	NOXA1
SCN8A	HPX	ADRB3	CYB5R1	ADIPOQ	RDH10	EGFR	PAK1	CCL24	CRHBP
HDAC2	SIX3	MAPK1	ACADS	MYL2	RHO	AKT2	SLC35F6	CACNA2D3	NOXO1
SLC13A1	LILRB1	EPM2A	ACOX1	PRDM16	THRA	PRPS1L1	ZNF398	HSD17B3	PLXNB3
OXCT2	MAP2K5	CNTN2	ACAD8	CKMT1B	DLX5	ANO9	DAP3	CFTR	MC5R
ASPH	FGF10	MAPK8IP2	GUK1	PPARG	OPN5	EME1	CPT2	ABHD6	MC1R
SUCLA2	FADD	ADCY5	NUDT12	FADS2	RS1	YWHAE	CALM3	DAGLA	F2R
SDHAF2	WNT2B	INSM1	ADK	ACSL4	CTSH	C1QBP	MTCH2	MGLL	AIF1
HIF1AN	TIRAP	ATP7A	POLB	SLC16A12	DHRS2	SPTBN1	PAGR1	FCER1A	PKP2
PLAT	ENPP6	PAM	IVD	PTGER4	CBR3	ACVR2B	CYBA	FCER1G	SOCS1
GRIN2A	IL6	NLRP11	CYB5R3	ABCC2	THRB	ID1	FHL1	CCR7	PPP2R1A
GRIN2B	NOD2	ATP8A1	ANKH	OPN3	CBR1	ABCG2	NR0B2	GPR55	SERPINE2
GPD1L	IL4	FGFR1	IMPDH2	SLC8B1	MTHFR	CLSPN	SMARCD3	C3	AFM
SUGCT	CHKA	NOS1	IMPDH1	PLA2R1	LSM8	VTCN1	PRADC1	PTGIR	PKP3
COLGALT2	FAS	PAH	TERT	MAP4K4	BHMT2	ANKRD6	IGSF21	BIN3	SEC14L6
SUOX	GABRD	SLC22A1	NQO2	OPN4	AHCYL2	MAPRE1	MED7	ZRANB3	JUP
CCL5	GABRE	PIK3R2	FDXR	PNPLA2	AHCYL1	MAPRE3	CCNC	RAC2	CCL3
ALDH9A1	GABRA4	GNB5	NQO1	CNST	MCEE	TIGAR	MAP3K1	CYBB	TTPA
CYP11A1	GABRB3	SYT2	ENPP3	SLC8A3	CEBPA	THBS1	KDM5A	PGRMC1	PRKCG
ACAT1	LTA	AVPR1A	ENPP1	HEG1	PCBD1	SOX18	PPP5C	TLR4	NF2
PNLIPRP2	SLC6A4	OXT	GSR	MYOD1	MRI1	LCN2	HSPE1	RAC1	DOCK5
DDC	SLC5A7	TESC	DPYD	SP3	WDHD1	OTC	TBP	NCF1	DOCK4
BCKDHB	SIRT2	PPP1R1B	IL4I1	SCD5	NDOR1	ACVR1C	MMS19	RAC3	NTSR1

Table 4: The target gene for diabetes obesity gene and SLBZS

Gene	Gene	Gene	Gene	Gene	Gene
SERPINE1	FADS1	THBS1	VIP	ASS1	GSTO1
UBE2B	CKB	DGAT2	IGF1	MMAB	TP53I3
SLC25A1	SERPINB7	ADAM17	SPARC	PDGFRL	ADAP2
ACADSB	PTGER2	UCHL1	ALDH1B1	NAPEPLD	TET1
ACSS2	S100A8	COPS5	APOE	PODXL	TNFAIP3
CHRNA7	RET	HEXIM1	TYMS	AOC3	LYZ
AHCY	SCD	PNRC2	ENPP3	RFWD3	FASN
KCNA1	FADS2	SULF2	GFER	GAS6	DNAJB9
SPX	SLC16A12	CFTR	ACACA	SLC16A10	CDKN1A
EPHX2	RRM2	GSTT1	CRYZ	CLSPN	

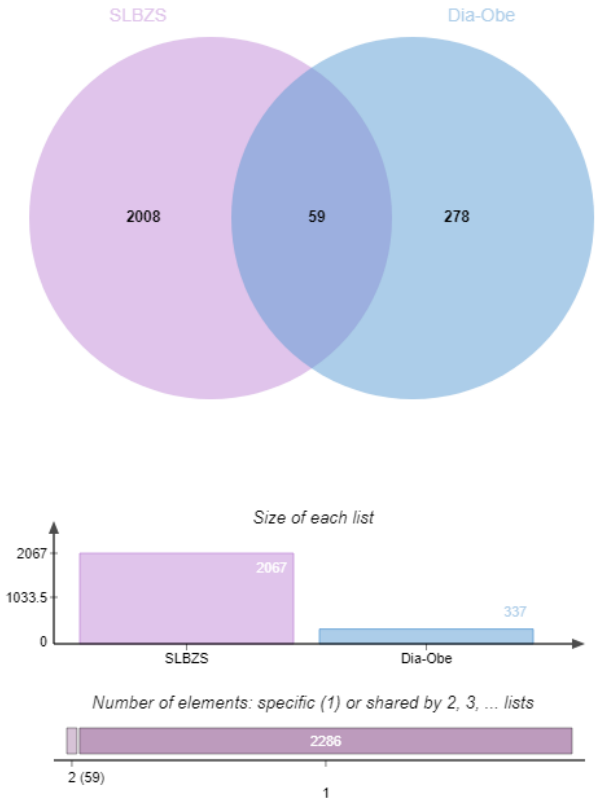

Fig. 11: The venn diagram of the target gene for diabetes obesity gene and SLBZS

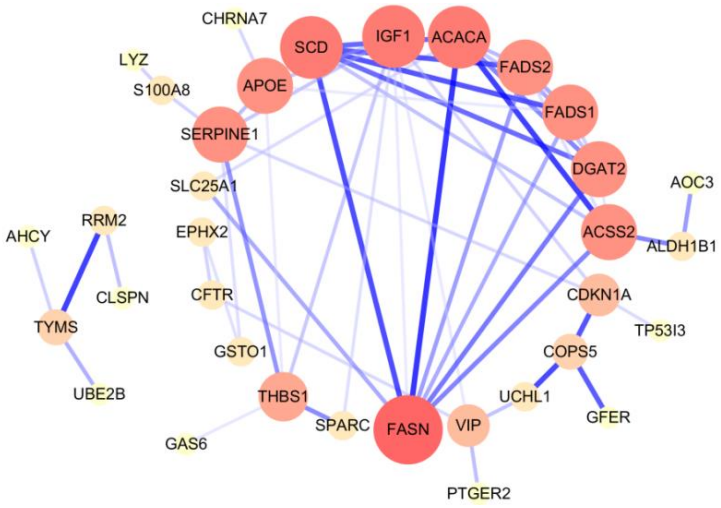

Fig. 12: PPI network of diabetic obesity related targets of SLBZS

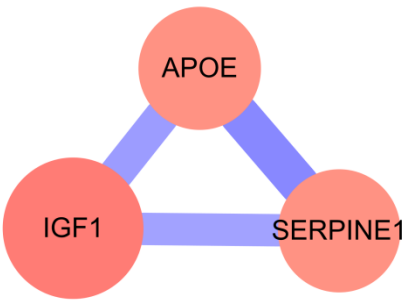

Fig. 13: 3 core targets were screened by cytoscape

Through the gene enrichment analysis function in String, 7 KEGG signal pathways related to the above 59 targets were found. See table 5 for details. Through the KEGG signal pathway analysis platform (https://www.genome.jp/kegg/pathway.html), it was found that SLBZS affects the production of fat by affecting the biosynthesis of unsaturated fatty acids (hsa01040) and fatty acid metabolism (hsa01212); reduce the conversion of sugar and fat by affecting the metabolic process of pyruvate (hsa00620); corrects the imbalance of energy metabolism by activating AMPK pathway (hsa04152) and metabolic pathway (hsa01100); up-regulates autophagy to promote the decomposition of adipose tissue by activating p53 pathway (hsa04115). The relationship between pyrimidine metabolic pathway (hsa00240) and the development of obesity remains unclear, however, the literature [20] compared the differences in metabolic pathways of adipose tissue around the tumor of obese mice and on the opposite side of the tumor of obese mice. It was found that many differential pathways were involved in carcinogenesis, such as purine and pyrimidine metabolism, which indicated that obesity might be potentially associated with the occurrence of some cancers.

Table 5: Related pathways of SLBZS in treating diabetic obesity

Pathway	Description
hsa01040	Biosynthesis of unsaturated fatty acids
hsa01212	Fatty acid metabolism
hsa04115	p53 signaling pathway
hsa00620	Pyruvate metabolism
hsa00240	Pyrimidine metabolism
hsa04152	AMPK signaling pathway
hsa01100	Metabolic pathways

Results of animal experiments

Establishment of diabetic obesity mouse model

The body weight and Lee's index of mice in high glucose and high fat diet group (HFD group) were significantly different from those in routine diet group (RD group) ($P<0.01$), as shown in table 4. After the modeling period, the body mass of HFD group was greater than or equal to the body mass of RD group mice ×120%, as shown in fig. 14. After modeling, the blood glucose of mice in HFD group was greater than or equal to the blood glucose of mice before modeling ×130%, as shown in fig. 15. Therefore, the diabetic obesity mouse model was successfully established.

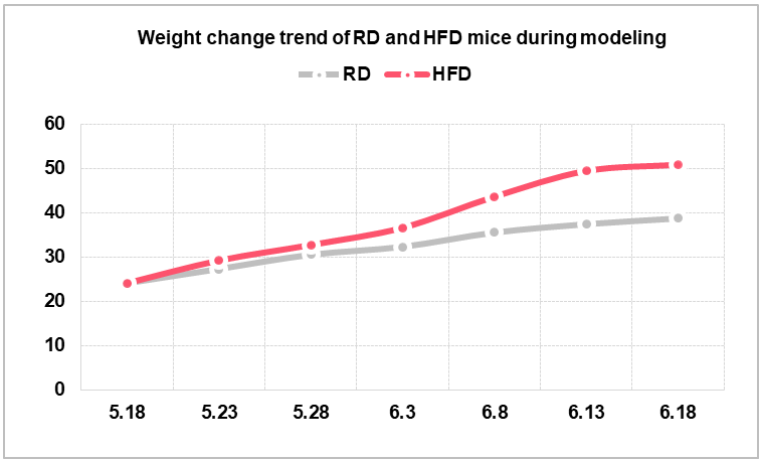

Fig. 14: Weight change trend of RD and HFD mice during modelling

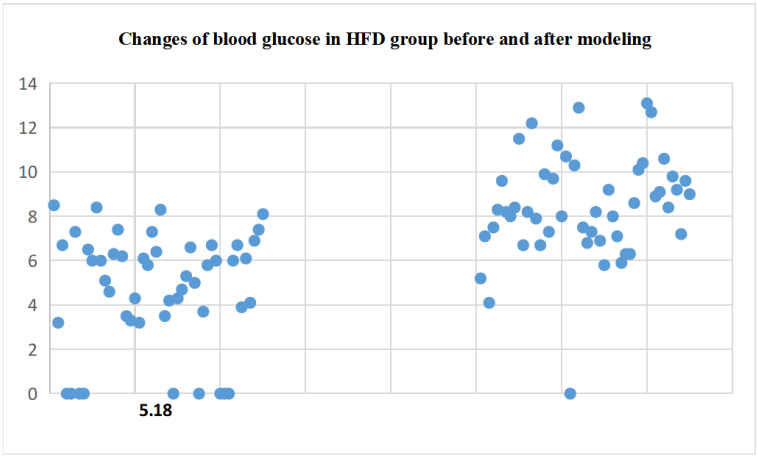

Fig. 15: Scatter diagram of blood glucose in HFD group before and after modelling

Results of blood glucose, body weight, body length and Lee's index of mice

The measurement results showed that compared with the HFD group, the weight of mice treated with SLBZS decreased significantly, while the decrease of blood glucose was not significant enough, as shown in fig. 16-17. After two weeks of intragastric administration of SLBZS, there was an extremely significant difference in body weight between obese mice and HFD group (P<0.01). In addition, there was a significant difference in Lee's index between low-dose administration group and high-dose administration group (P<0.05), but there was no significant difference in body length between groups; see table 6 for details. The results showed that SLBZS has a significant effect on reducing the body mass and Lee's index of diabetic obesity mice and is positively correlated with the dose. The effect of SLBZS on the blood glucose of mice needs further verification.

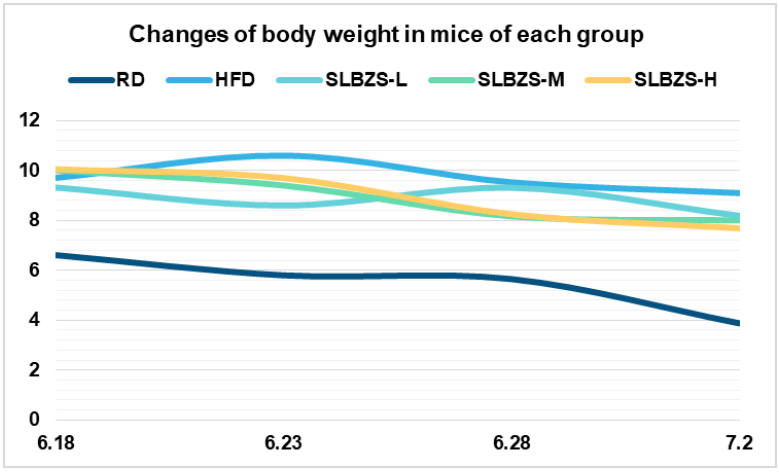

Fig. 16: Change of body weight in mice of each group

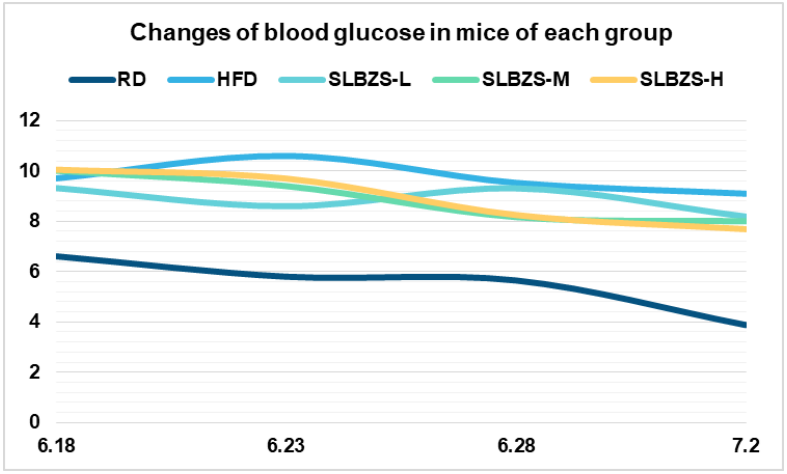

Fig. 17: Change of blood glucose in mice of each group

Table 6: Comparison of weight, body length and Lee's index of mice in each group ($\overline{X} \pm S$, n=6)

Group	Body weight (g)	Body length (cm)	Lee's index
RD	43.08±1.54[a]	10.6±0.19	3.3±0.072[a]
HFD	53.12±3.1	10.75±0.46	3.5±0.11
SLBZS-L	47.35±2.03[a]	10.95±0.47	3.3±0.11[b]
SLBZS-M	45.18±2.91[a]	10.61±0.42	3.36±0.12
SLBZS-H	47.4±1.52[a]	10.98±0.36	3.3±0.074[a]

(Note: P values are compared with HFD group, a indicates P<0.01, b indicates P<0.05)

Results of HE staining analysis

HE-stained photographs of adipose tissue of mice in each group were observed, as shown in fig. 18. Compared with the blank group, the adipose volume of the model group was significantly larger than that of the blank group. Compared with the model group, the adipose volume of in the low-dose group decreased, while the adipose volume of in the middle and high-dose groups decreased significantly. Therefore, SLBZS had a significant effect on reducing the adipose volume of diabetic obesity mice.

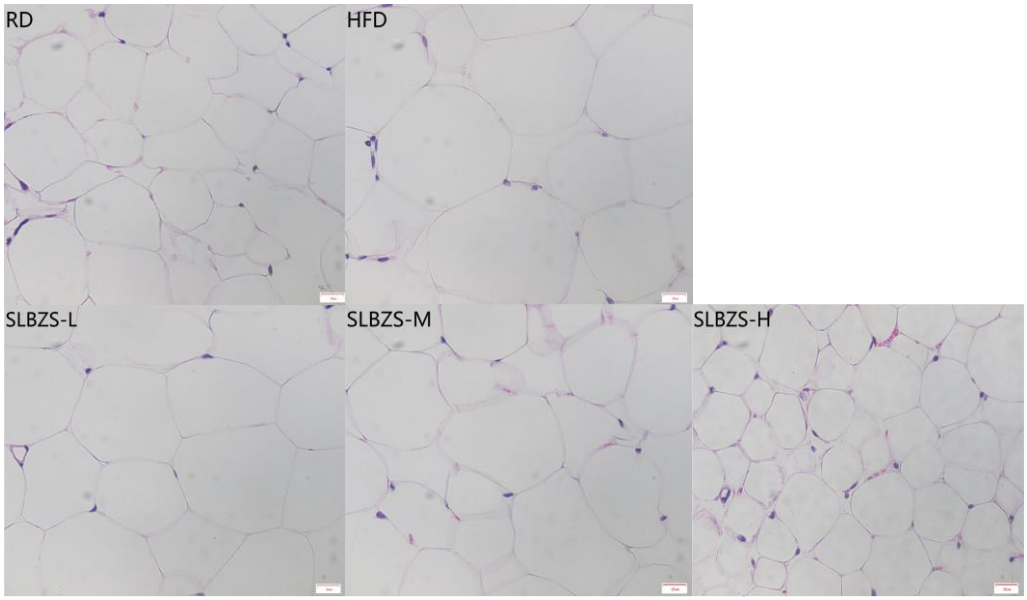

Fig. 18: HE staining photos of adipose tissue of mice in each group under 400X microscope

Results of blood lipid analysis

The content of cholesterol (TC) and triglyceride (TG) in serum was measured by microplate colorimetry, and the calculation formula was as follows:

$$\text{Cholesterol (mmol/l)} = \frac{\text{Sample OD value} - \text{blank OD value}}{\text{Calibrated OD value} - \text{blank OD value}} \times \text{Calibrator concentration (5.17 mmol/l)}$$

$$\text{Triglyceride (mmol/l)} = \frac{\text{Sample OD value} - \text{blank OD value}}{\text{Calibrated OD value} - \text{blank OD value}} \times \text{Calibrator concentration (2.26 mmol/l)}$$

The results showed that there were significant differences in cholesterol and triglyceride between HFD mice and RD mice, which indicated that TG and TC of mice fed with high sugar and high fat were significantly increased. However, the TC and TG of mice treated with SLBZS showed a downward trend, and the higher the dose, the more significant the decrease was. Compared with HFD mice, the difference between TC and TG in middle and high dose groups was extremely significant, while that in low dose group was not significant, as shown in table 7 for details.

Table 7: Concentration of cholesterol and triglyceride in mice of each group（$\overline{X} \pm S$, n=6）

	RD (mmol/l)	HFD (mmol/l)	SLBZS-L (mmol/l)	SLBZS-M (mmol/l)	SLBZS-H (mmol/l)
TG	0.615±0.083[a]	1.216±0.146	1.072±0.065	0.817±0.0472[a]	0.808±0.085[a]
TC	2.287±0.356[a]	3.317±0.46	3.260±0.46	2.60±0.27[b]	2.405±0.196[a]

(Note: P values are compared with HFD group, a indicates P<0.01, b indicates P<0.05)

Results of core target analysis

Elisa results showed that compared with RD mice, the concentrations of APO-E, IGF-1 and PAI-1 in serum of HFD group were significantly different, which indicated that the levels of APO-E, IGF-1 and PAI-1 in serum of mice fed with high sugar and high fat were significantly increased. The mice treated with SLBZS showed significantly down-regulated levels of APO-E, IGF-1 and PAI-1 in serum, and the higher the dose, the more significant the decrease was. Compared with HFD mice, the differences of APO-E, IGF-1 and PAI-1 in middle and high-dose groups were significant, while those in low dose groups were not significant, as shown in table 8.

Table 8: Protein concentrations of Apo-E, IGF-1 and PAI-1 in serum of mice in each group（$\overline{X} \pm S$, n=6）

Key target gene	RD	HFD	SLBZS-L	SLBZS-M	SLBZS-H
APO-E (μg/ml)	42.45±3.343[a]	62.62±5.604	64.49±6.593	52.65±5.66[b]	47.24±4.038[a]
IGF-1 (ng/ml)	38.39±2.763[a]	63.93±4.803	63.55±5.575	55.81±4.734[b]	42.95±1.925[a]
PAI-1 (ng/ml)	15.37±1.182[a]	26.35±4.135	24.21±3.239[b]	20.70±2.0[a]	19.10±2.802[a]

(Note: P values are compared with HFD group, a indicates P<0.01, b indicates P<0.05)

DISCUSSION

SLBZS, first recorded in the book "Taiping Huimin Heju prescription" of the Song Dynasty, has been an important prescription for the treatment of spleen and stomach deficiency and difficult diet since ancient times. The administration of SLBZS is capable of dispelling the pathological products formed by spleen's unhealthy movement, and making the patient's qi and blood smooth, viscera soft and obesity disappear [21]. Traditional Chinese medicine has a long history of treating phlegm-dampness obesity with SLBZS, however, there is still a lack of systematic and quantitative scientific data to comprehensively evaluate its therapeutic effect. Meta-analysis verified that SLBZS could significantly reduce BMI index, HbA1c, 2 hPG, FBG, Homa-IR and waist-hip ratio of diabetic obese patients. Based on the above-mentioned results, we established an animal experiment to verify the therapeutic effect of SLBZS on diabetic obesity mice. The results showed that the adipose cells of mice treated with SLBZS were significantly reduced, and the body weight,

Lee's index, triglyceride and cholesterol of mice were significantly decreased, which confirmed that SLBZS had a definite therapeutic effect on obesity. However, the influence of experimental results on blood glucose of mice remained clear, which might be related to short modeling time, insufficient damage of islet β cells and unstable fluctuation of blood glucose. The results of the present study were able to provide strong evidence for the clinical application of SLBZS in the treatment of diabetic obesity.

In addition, to further analyze the mechanism of SLBZS in the treatment of diabetic obesity, we predicted its related signal pathways and core targets through network pharmacology. The results showed that the mechanism of SLBZS in treating diabetic obesity may be related to influencing the synthesis of unsaturated fatty acids and fatty acids, reducing the transformation of sugar and fat, correcting the imbalance of energy metabolism, and promoting the decomposition of adipose tissue by up-regulating autophagy. The animal experimental results also illustrated that SLBZS had significant regulatory effects on three core targets, which provided a useful reference for us to further reveal the mechanism of SLBZS in treating diabetic obesity.

FUNDING

National Natural Science Foundation(Grant No. 81660727);Natural Science Foundation of Jiangxi Province (Grant No. 20192BAB205095);1050 Young Talents Project of Jiangxi University of Traditional Chinese Medicine (Grant No. 5141900102);Science and technology planning project of Jiangxi Administration of traditional Chinese Medicine(Grant No.2020A0320);Startup fund for doctoral research of Jiangxi University of traditional Chinese Medicine(Grant No.2020BSZR017)

AUTHORS CONTRIBUTIONS

Diyao Wu took charge of guiding the experiments and paper writing. Xiaoling Zhou wrote the manuscript and finished data mining research. Liping Tang completed the experimental design and execution. Xinyou Zhang made the design research and provided fund support.

CONFLICT OF INTERESTS

There is no conflict of interest

REFERENCES

1. Dajin Z, Zheng Z, Nan JL. China expert consensus on relieving type 2 diabetes mellitus. Chin Gen Pract. 2021;24(32):4037-48.
2. Xukai W, Peng C. Is insulin resistance the cause or result of hypertension? Chin J Hypertens. 2020;28(04):302-7.
3. Yuan X. Thoughts and methods of traditional Chinese medicine in the treatment of metabolic syndrome. J Trad Chin Med. 2003;4:301-2.
4. Pingping B, Chunxiao W. Cancer prevalence and prevention practice in shanghai. Shanghai Prev Med. 2020;32(11):955-62.
5. NG M, Fleming T, Robinson M, Thomson B, Graetz N, Margono C. Global regional and national prevalence of overweight and obesity in children and adults during 1980-2013: a systematic analysis for the global burden of disease study 2013. Lancet. 2014;384(9945):766-81. doi: 10.1016/S0140-6736(14)60460-8, PMID 24880830.
6. Zhou Q, Chang B, Chen XY, Zhou SP, Zhen Z, Zhang LL. Chinese herbal medicine for obesity: a randomized double blinded multicenter prospective trial. Am J Chin Med. 2014;42(6):1345-56. doi: 10.1142/S0192415X14500840, PMID 25406653.
7. Yao Q, LI S, Cheng X, Zou Y, Shen Y, Zhang S, Yin Zhi Huang. A traditional Chinese herbal formula ameliorates diet induced obesity and hepatic steatosis by activating the AMPK/SREBP-1 and the AMPK/ACC/CPT1A pathways. Ann Transl Med. 2020;8(5):231. doi: 10.21037/atm.2020.01.31, PMID 32309378.
8. Zhang Y, Tang K, Deng Y, Chen R, Liang S, Xie H. Effects of shenling baizhu powder herbal formula on intestinal microbiota in high fat diet induced NAFLD rats. Biomed Pharmacother. 2018 Jun;102:1025-36. doi: 10.1016/j.biopha.2018.03.158, PMID 29710519.
9. Lili T, Huiying W, Xiaoping C, sang Xia, Zeng Cheng, Xin Jun, Liu Guiying, Niu Xinyi. Effect of acupoint catgut embedding combined with spleen strengthening and expectorant traditional Chinese medicine on glucose and lipid metabolism in obese patients with polycystic ovary syndrome. J Trad Chin Med. 2010;51(03):239-42.
10. Guideline for prevention and treatment of type 2 diabetes in China 2017 Edition) [J]. China Journal of Practical Internal Medicine. 2018,38(04):292-344.
11. Junhua P, Suohua G, Huanyan Z. Effects of shen ling baizhu powder combined with metformin on miR-146a, GLP-1 and blood lipids in obese patients with type 2 diabetes mellitus. Tianjin Med. 2021;49(02):203-7.
12. Haiyan J, Suohua G, Xue Y. Effects of shen ling baizhu powder combined with metformin on intestinal flora in obese diabetic patients and their adverse reactions. Gansu J Sci. 2020;32(06):9-13.
13. Luyang S, Huanyan Z, Xue Y. Shen ling baizhu powder combined with metformin in treatment of obese patients with type 2 diabetes miR-221 MCP-1 TNF-α. Clin Lab. 2020;38(09):710-3.
14. Xiaoshan H. Integrated traditional Chinese and Western medicine in the treatment of obesity type 2 diabetes. J Diet Health Care. 2020;7:79.
15. Zhifang C. Shen ling baizhu powder in the treatment of obesity type 2 diabetes mellitus with spleen deficiency and dampness syndrome. Clinical Medical Literature Electronic Magazine. 2019;6(03):155-6.
16. Ningning M. Shen ling baizhu powder in the treatment of obesity type 2 diabetes mellitus with spleen deficiency and dampness syndrome. Chinese Medicine Guide. 2017;23(12):74-6.
17. Fujian C, Cuiling Z. Clinical study on the treatment of obesity type 2 diabetes with integrated traditional Chinese and Western medicine. Chin J Trad Chin Med. 2016;31(11):1688-90.
18. Xiaojuan X, Dan L, Jing W. Adjuvant treatment of 80 cases of type 2 diabetes mellitus with obesity by shen ling baizhu san. Hainan Med. 2015;26(24):3612-4.
19. Xiu M. Modified shen ling baizhu powder for the treatment of obesity with spleen deficiency and dampness syndrome in early stage of diabetes. J Chin Med Clin J. 2015;27(11):1583-5.
20. Maguire OA, Ackerman SE, Szwed SK, Maganti AV, Marchildon F, Huang X. Creatine mediated crosstalk between adipocytes and cancer cells regulates obesity driven breast cancer. Cell Metab. 2021;33(3):499-512. doi: 10.1016/j.cmet.2021.01.018, PMID 33596409.
21. Likun D, Cuicui L. Exploring the mechanism of treating obesity from the spleen from autophagy. Chin J Trad Chin Med. 2020;35(11):5707-9.